Contractile force generation by 3D hiPSC-derived cardiac tissues is enhanced by rapid establishment of cellular interconnection in matrix with muscle-mimicking stiffness

Soah Lee[1,+], **Vahid Serpooshan**[2,+], **Xinming Tong**[3], **Sneha Venkatraman**[2,4], **Meelim Lee**[5], **Jaecheol Lee**[2,6,7], **Orlando Chirikian**[2,4], **Joseph C. Wu**[2,6,7], **Sean M. Wu**[2,6,7,*], and **Fan Yang**[3,5,*]

[1]Department of Materials Science and Engineering, Stanford University, Stanford, CA

[2]Stanford Cardiovascular Institute, Stanford University School of Medicine, Stanford, CA

[3]Department of Orthopedic Surgery, Stanford, CA

[4]Biology Program, California State University Channel Islands, Camarillo, CA

[5]Department of Bioengineering, Stanford University, Stanford, CA

[6]Institute of Stem Cell Biology and Regenerative Medicine, Stanford, CA

[7]Department of Medicine, Division of Cardiovascular Medicine, Stanford University, Stanford, CA

Abstract

Engineering 3D human cardiac tissues is of great importance for therapeutic and pharmaceutical applications. As cardiac tissue substitutes, extracellular matrix-derived hydrogels have been widely explored. However, they exhibit premature degradation and their stiffness is often orders of magnitude lower than that of native cardiac tissue. There are no reports on establishing interconnected cardiomyocytes in 3D hydrogels at physiologically-relevant cell density and matrix stiffness. Here we bioengineer human cardiac microtissues by encapsulating human induced pluripotent stem cell-derived cardiomyocytes (hiPSC-CMs) in chemically-crosslinked gelatin hydrogels (1.25×10^8/mL) with tunable stiffness and degradation. In comparison to the cells in high stiffness (16 kPa)/slow degrading hydrogels, hiPSC-CMs in low stiffness (2 kPa)/fast degrading and intermediate stiffness (9 kPa)/intermediate degrading hydrogels exhibit increased intercellular

*Address for correspondence: Sean M. Wu, M.D. Ph.D., G1120A Lokey Stem Cell Building, 265 Campus Drive, Stanford, CA 94305, USA, Phone: 650-724-4498, Fax: 650-724-4689, smwu@stanford.edu; Fan Yang, Ph.D., Departments of Orthopedic Surgery and Bioengineering, Stanford University School of Medicine, 300 Pasteur Dr, Edwards R105, Stanford, CA 94305, USA, Phone: 650-725-7128, Fax: 650-723-9370, fanyang@stanford.edu.
+Authors contributed equally.

Data is normalized to GAPDH and further normalized to the 2 kPa group. Data presented as mean ± s.e.m. statistical analysis done by Tukey's Multiple Comparisons one-way ANOVA. (n.s. $p > 0.05$, n=3)

Author Contributions
X.T. synthesized materials and performed ^{1}H-NMR analysis. V.S. and S.V. performed hiPSC-CM differentiation. S.L. performed materials characterization, hiPSC-CM encapsulation, culture, and assays in 3D, including viability, metabolic activity, and optical microscopy. S.L., M.L., and V.S. carried out immunohistochemistry analysis. S.L. performed imaging-based functionality assay. S.L., V.S., S.M.W., and F.Y. conceptualized the project goals, designed all experiments, reviewed the data acquired, and prepared the manuscript.

Competing Financial Interests statement
None

network formation, α-actinin and connexin-43 expression, and contraction velocity. Only the 9 kPa microtissues exhibit organized sarcomeric structure and significantly increased contractile stress. This demonstrates that muscle-mimicking stiffness together with robust cellular interconnection contributes to enhancement in sarcomeric organization and contractile function of the engineered cardiac tissue. This study highlights the importance of intercellular connectivity and physiologically-relevant cell density and matrix stiffness to best support 3D cardiac tissue engineering.

Keywords

human induced pluripotent stem cell-derived cardiomyocytes; cardiac tissue engineering; gelatin hydrogels; stiffness; degradation

1. Introduction

Coronary heart disease and the associated myocardial infarction are the leading causes of death in the US and globally. In 2013, coronary heart disease alone caused ~1 of every 7 deaths in the US[1]. Following the damage to myocardium, human heart exhibits deficient ability to restore its function due to limited self-renewal capacity of adult cardiomyocytes (CMs). Current treatment modalities for loss of heart function include supplementation of therapeutic products, surgical reconstruction, implantable devices, or ultimately organ transplantation[2, 3]. Although these conventional treatments have shown some efficacy and improved the quality of life for the patients, they cannot effectively regenerate the damaged heart tissue and restore its function. Clinical trials of cell transplantation have shown promise to replace the dead cells and restore the impaired function of heart. However, the efficacy of cell transplantation has been controversial mainly due to poor cell viability, retention, and engraftment[4–10]. Therefore, it is crucial to develop more reliable and reproducible methods to deliver therapeutic cells.

To enhance cell-based therapies for cardiac repair, tissue engineering approaches have been utilized to engineer 3D cardiac tissues by encapsulating the therapeutic cells into 3D hydrogels for aiding cell delivery, viability, and functionality. To engineer physiologically relevant 3D cardiac tissue, choices of cell source and the scaffolding materials are of great importance. Given the cardiac tissue is characterized by high cell concentration ($10^8 – 10^9$ cells/mL)[11], reliable source of CMs is critical. Human induced pluripotent stem cells (hiPSCs) have emerged as an attractive source of human CMs since they can self-renew indefinitely and be directed towards CM differentiation efficiently (80 – 90%). Furthermore, the cardiomyocytes generated can be patient-specific[12]. Despite its attractiveness, very few studies have tried to engineer 3D cardiac tissue using hiPSC-derived CMs (hiPSC-CMs). In these studies, hiPSC-CMs were encapsulated within extracellular matrix (ECM)-derived 3D hydrogels including Matrigel, type I collagen and fibrin[13–15]. While ECM-derived hydrogels have shown some promise for engineering structurally cardiac-mimetic tissues, the major limitations of these hydrogels are weak mechanical strength/stiffness and undesirable premature degradation before sufficient new matrix production. Since heart is pulsatile environment, the engineered cardiac tissue requires robust mechanical integrity and

stability. In addition, it is essential to match the hydrogel stiffness to that of native cardiac tissue (8 – 11 kPa), given matrix stiffness has been shown to play an important role in maturation of muscle[16, 17]. However, natural ECM hydrogels are often physically crosslinked and exhibit stiffness in a range of 0.01 – 1 kPa, which is one- to three-orders of magnitude lower than the mechanical environment of cardiac tissue[18–20]. Moreover, degradation of the hydrogel scaffolds must be in balance with formation of sufficient cellular connections and new matrix deposition by the encapsulated cells, since densely connected CMs are responsible for electrical signal propagation and synchronized heart beating. Previous studies reported that fibrin gels prematurely degrade within 1–2 days, which requires supplementation of fibrinolysis inhibitor in culture to delay the degradation[14]. Taken together, there is a clear need for a new biomaterials platform where mechanical stiffness and degradation rate of the hydrogels can be varied in controlled manner for hiPSC-CM based cardiac tissue engineering.

Here, we demonstrate bioengineering of human cardiac microtissues using chemically-crosslinked gelatin hydrogels with enhanced stiffness and tunable degradation properties, obtained by functionalizing the gelatin polymer with different degrees of vinyl sulfone (VS) groups. The effects of varying hydrogel stiffness and degradation on cardiac tissue formation by hiPSC-CMs were evaluated by encapsulating cells at physiologically-relevant density (125M cells/mL). Outcomes were evaluated by characterizing cell survival as well as structural organization and contractile function of newly formed cardiac tissues.

2. Results

2.1. Gelatin hydrogels with tunable stiffness and degradation rate supported robust hiPSC-CM survival

To modulate stiffness and degradation rate of gelatin hydrogel, hydrogel crosslinking density was changed by varying degree of VS functionalization on gelatin polymer chains (Fig. 1a). To mimic cell-dense cardiac tissue, hiPSC-CMs were encapsulated at physiologically relevant density (125M cells/mL) in gelatin hydrogels and cultured for 14 days in differentiation media (Fig. 1b,c). The degree of VS functionalization was tuned by varying the reaction time (0.5 – 2 h) of gelatin with divinyl sulfone. ^{1}H-NMR data confirmed that gelatin was functionalized with VS at three different degree of functionalization, low, intermediate, and high, respectively (Fig. 2a). To validate that degree of functionalization can change degradation rate of gelatin hydrogels, *in vitro* degradation test of acellular gelatin hydrogels was conducted using collagenase IV solution. We found that the hydrogels made from low VS functionalized gelatins resulted in the fastest degradation, whereas the one made from high VS functionalized gelatins resulted in the slowest degradation (Fig. 2b). Since hydrogel crosslinking density can modulate *not only* hydrogel degradation rate *but also* stiffness, uniaxial compression test was conducted to investigate the effect of varying VS degree on stiffness of gelatin hydrogels. Uniaxial compression test revealed that increasing degree of VS functionalization increased hydrogel stiffness (Fig. 2c). Next, to evaluate cytotoxicity of the materials and encapsulation process, cell viability and metabolic activity were examined using Live/Dead and AlamarBlue assays. Cells were highly viable within all hydrogel groups 1 day after the encapsulation and throughout 14 days of culture

(Fig. 2d). Cell viability remained unaffected in the mid-portion of hydrogels at day 14 (Fig. S4 and Video S4–6). Furthermore, cellular metabolic activity at day 1 showed no significant differences between all three groups and 2D control group (Fig. 2e).

2.2. Increasing degradation rate or decreasing stiffness of gelatin hydrogels facilitated intercellular network formation

Since cardiac tissue is characterized by high cellularity and interconnectivity, intercellular network formation was examined over the culture period by bright field images (Fig. 3). At day 1, hiPSC-CMs were homogeneously encapsulated and distributed as single cells within all gelatin hydrogel groups. By day 3, hiPSC-CMs in 2 and 9 kPa groups became aggregated to form intercellular network, while those in 16 kPa groups still mostly remained isolated. By day 7, it was clearly shown that decreasing stiffness or increasing degradation accelerated intercellular network formation. In particular, hiPSC-CMs in 2 kPa hydrogel groups, formed thick honey-comb-like structure.

2.3. Gelatin hydrogels with muscle-mimicking stiffness and intermediate degradation, promoted sarcomeric organization and contractile function of the encapsulated hiPSC-CMs

To assess effects of varying hydrogel stiffness and degradation on structure and function of the engineered cardiac tissues, expressions of contractile machinery protein (α-actinin) and intercellular junction protein (connexin 43) were examined. We found that hiPSC-CMs in 2 and 9 kPa groups, expressed significantly higher level of α-actinin in comparison to those in 16 kPa hydrogel (Fig. 4a,b). Interestingly, only the hiPSC-CMs encapsulated in 9 kPa hydrogels showed organized sarcomeric α-actinin structure.

Since matrix remodeling and *de novo* ECM production is crucial in new tissue formation, we further investigated effects of stiffness and degradation rate on *de novo* production of elastin, an ECM protein that *only* mature CMs produce.[21] We found that elastin production of hiPSC-CMs was significantly increased with decreasing matrix stiffness (Fig. 4c,d).

Finally, to investigate effects of stiffness and degradation rate on functionality of the engineered cardiac tissues, global contraction behavior of the tissues was evaluated by imaging-based computational analysis. Particle imaging velocimetry algorithm enabled extracting displacement vector fields from hiPSC-CM beating videos (Fig. 5a, Video S1–3). Heat maps of displacement fields correspond well to the hydrogel contraction/relaxation behaviors, validating the particle imaging velocimetry algorithm (Video S1–3). Max displacement images are heat maps of the calculated displacement vector field when each engineered construct contracts or relaxes at maximum. Then, the maximum displacement velocity was plotted as a function of time (Fig. 5b). Maximum contraction/relaxation velocity was shown to be significantly higher in 2 and 9 kPa hydrogels than 16 kPa hydrogels (Fig. 5c, Fig. S1). In addition, the beating rate of the engineered tissue was calculated as an inverse of time interval between consecutive contraction peaks or relaxation peaks. It is notable that beating rate of 9 kPa hydrogels was significantly lower than the other groups (Fig. 5d). To evaluate how much force (*i.e.*, stress) hiPSC-CMs generate within the three different hydrogel groups, maximum contractile stress was calculated as a function

of the maximum contraction displacement and hydrogel stiffness. We found that cells in 9 kPa hydrogel groups generated the greatest contraction stress (374 ± 19 Pa) among all hydrogel groups (Fig. 5e).

3. Discussion

While encapsulation of CMs in 3D engineered constructs has been previously reported[22–24], the work presented here offers multiple distinct advantages. The hydrogel system used in our study enables precise tunability of mechanical properties of the 3D matrix. In particular, the range of stiffness used in this study (2 – 16 kPa) is significantly greater than that of ECM-derived hydrogels used in previous studies (e.g. 0.01 – 1 kPa for collagen and fibrin) [13–15, 20, 25, 26], leading to greater force generation in our study. Moreover, tunable degradability of the hydrogel system used in this study allows for culturing of cardiomyocytes for 14 days without supplementation of enzyme inhibitors that delay the degradation used in previous studies[14, 15, 20, 25–27]. Encapsulating CMs at physiologically-relevant cell densities and *in-depth* evaluation of their viability and function for longer periods of 3D culture have also been challenging. While most of published reports used remarkably lower cell densities (e.g. 0.2 – 10M cells/mL) than the observed *in vivo*[23, 29], we encapsulated hiPSC-CMs in gelatin hydrogels at physiologically-relevant density (125M cells/mL) and showed high cell viability and function during 14 days of culture.

By encapsulating physiologically-relevant concentration of hiPSC-CMs in hydrogel with varying stiffness and degradation, we show that the hydrogel with myocardium-mimicking stiffness (9 kPa) and intermediate degradation best promotes hiPSC-CM connectivity, sarcomeric organization, and contractile function in 3D. Interestingly, sarcomeric organization of hiPSC-CMs in 3D was only observed in 9 kPa hydrogel group. hiPSC-CMs in 2 kPa and 16 kPa groups showed minimal evidence of sarcomeric organization despite the presence of intercellular network formation (Fig. 4). Furthermore, enhancement in sarcomeric organization led to significantly greater contractile force (i.e. stress) generation by the engineered tissues (Fig. 5). This agrees with previous study where organization of α-actinin into sarcomeric structure and high levels of gap junction expression are required for generating physiologically relevant contractile force in the cardiac tissues[30]. In previous 3D human cardiac tissue engineering studies, it has been reported that hiPSC-CMs encapsulated in collagen hydrogel, generated contractile stress levels ranging from 12 Pa (without mechanical stimulation) to 80 Pa (with mechanical stimulation)[15]. In our study, hiPSC-CMs in 9 kPa hydrogels generated ~ 30 times greater contractile stress (373.5 Pa) without any mechanical stimulation. Although contractile stress of our engineered cardiac tissues is still much lower than that of intact heart muscle (40 – 80 kPa)[31], this is significant enhancement by mimicking matrix stiffness and cell density to that of heart muscle tissue. We believe a further increase in contractile force can be achieved by aligning hiPSC-CMs in a directional manner using different casting method or with mechanical/electrical stimulation[32–34].

With regards to the role of matrix stiffness in promoting hiPSC-CM maturation, our data demonstrate that matrix stiffness can facilitate sarcomeric protein organization and enhance contractile force generation without having to mature individual CMs. While many previous

studies have shown to facilitate maturation of CMs by mimicking 2D substrate stiffness to that of myocardium [16, 35–38], CM maturation has often been assessed by histological and functional analysis. In agreement with previous reports, our data showed stiffness-induced improvements in sarcomeric protein organization and contractile force generation. However, when maturation markers of hiPSC-CMs (TNNI3, TNNI3/TNNI1, GJA1) were evaluated[39], there were no statistically significant differences in cardiac maturation markers at mRNA level, suggesting that the observed structural/functional enhancement is not attributed to the maturation of hiPSC-CMs (Fig. S4). This highlights the importance of matrix properties in enhancing structure/function of the engineered cardiac tissue. At the same time, this study raises an important caveat regarding the frequent use of histological and functional analysis to imply changes in the maturity of hiPSC-CM without confirmatory data from gene expression analysis.

Here, we present a thiol-vinyl sulfone chemistry-based chemically crosslinked gelatin hydrogel platform that supports hiPSC-CM survival by varying the hydrogel crosslinking density. Thiol-vinyl sulfone chemistry has been widely used to encapsulate various cell types in hydrogels and has shown minimal cytotoxicity[40–42]. We show that chemically crosslinked gelatin hydrogels via thiol-vinyl sulfone groups supported high viability of hiPSC-CMs and metabolic activity comparable to that of CMs cultured on 2D (Fig. 2d,e). It is possible that the greater amount of unreacted thiol-containing crosslinkers in the 2 and 9 kPa hydrogel groups may lead to greater cytotoxicity, however, we believe that potential cytotoxicity of unreacted crosslinkers is marginal, since viability and metabolic activity of hiPSC-CMs in 2 and 9 kPa groups are as high as or even higher than those in 16 kPa group (Fig. 2 and S2). Within the two-week study period, encapsulated CMs in all groups showed an increase in metabolic activity, followed by a plateau (Fig. S2). Z-stack images of LIVE/DEAD stained 3D hydrogels demonstrated a relatively uniform CM viability and interconnectivity within the entire thickness of constructs in each study group, indicating that there has been no significant limitation on the oxygen/nutrient diffusion in the constructs (Fig. S3, Video S4–6). Uniform cell viability within these relatively thick 3D constructs can be attributed to the partial degradation of matrices which generates a highly porous structure that facilitate the diffusion of nutrients and oxygen into the engineered constructs.

To highlight distinct degradation profiles of the three hydrogel groups within a short time interval, we used greater concentration of collagenase IV in the *in vitro* degradation test (2 U/mL = 12.5 μg/mL, Fig. 2b), in comparison to the levels of cell-secreted MMPs in *in vitro* cell cultures (*e.g.*, 1–500 ng/mL)[43, 44]. Within the 2-week *in vitro* study period, cell-induced degradation of 16 kPa and 9 kPa hydrogels led to macroscopically intact tissue constructs, while the 2 kPa group showed some evidence of degradation, forming macroscopic pores within the constructs (Fig. 5a, Video S1–3). However, continuous secretion of ECM proteins by encapsulated hiPSC-CMs partly compensated the hydrogel degradation (Fig. 4c). Future studies will address the long-term durability of the engineered constructs for potential application *in vivo*. Several previous studies have conducted either long-term (up to 26 weeks) degradation tests by incubating tissue engineering scaffolds, with or without cells, in biologically related media (*e.g.*, PBS or culture media), or short-term enzymatic degradation assays[45–47]. For example, incubating gelatin-chitosan

hydrogels in PBS for 5 weeks resulted in ~45% degradation of hydrogels, while incubating with lysozyme degraded up to 95% of the constructs[45]. In another study, addition of 10 and 20 U/mL collagenase to collagen-hyaluronic acid-gelatin hydrogels immersed in PBS resulted in rapid (3–hr) degradation of the scaffolds to ~55 and 92%, respectively[48]. Given the significant differences that are often observed between *in vitro* and *in vivo* degradation behaviors of hydrogels, the potential use of these 3D constructs as a cardiac patch for cell delivery and tissue regeneration *in vivo* will require further *in vitro* studies at biologically-relevant MMP concentrations for longer time periods and *in vivo* studies.

We believe that CM interconnection in 3D must precede to enable sarcomeric protein re-organization and global contractile function of the engineered 3D construct. Intercellular connectivity of hiPSC-CMs is influenced by hydrogel crosslinking density that determines both hydrogel stiffness and degradation rate. However, we believe that degradation rate may play a bigger role in enabling cellular interconnection because chemically-crosslinked hydrogel is often nano-porous and the pore size difference induced by varying hydrogel stiffness may not be significant to influence intercellular connectivity. For example, the pore size difference between 2 kPa and 16 kPa hydrogels would be only a few nanometers [49]. To further validate which element plays a more crucial role, biomaterials system that enables independent control of stiffness and degradation should be employed [50].

Electromechanical coupling of the engineered cardiac tissues is critical for directional signal propagation and synchronized contraction. While this study demonstrates global contraction of the engineered construct, suggesting electromechanical coupling of the cardiomyocytes (Video S1 – 3), direct evaluation of electrical coupling of the interconnected cardiomyocytes has not been done. In future studies, propagations of calcium transient and action potential need to be measured to further examine conduction velocity/directionality of the engineered constructs and synchronization of contraction[52, 53].

4. Conclusion

In summary, we demonstrate that chemically crosslinked gelatin hydrogel serves as an important materials platform for hiPSC-CM-based cardiac tissue engineering by enabling control of intercellular connection and enhancing mechanical stability. Our data demonstrate that matrix properties (i.e. stiffness and degradation) are sufficient to promote sarcomeric organization and contractile function of the engineered cardiac tissue construct. The resulting bioengineered cardiac construct can be broadly applicable as a physiologically-relevant 3D *in vitro* tissue model to study cardiac development, cardiac diseases, and drug screening.

5. Experimental Section

5.1. Synthesis of gelatin-vinyl sulfone and 4-arm poly(ethylene glycol)-thiol

Gelatin (Sigma, G9391) was converted into gelatin-vinyl sulfone (VS) by reacting with divinyl sulfone (Sigma) Na_2CO_3 buffer (1 M). To vary VS functionality, the reaction time was varied as 0.5, 1.0, 2.0 hours, resulting in low, intermediate and high functionality, respectively. The reaction was stopped by neutralizing the solution with concentrated HCl

solution. 4-arm poly(ethylene glycol) (PEG) (MW 10 kDa, JenKem) was converted into 4-arm-PEG-amine by reacting with phthalimide (Sigma) catalyzed by diisopropyl azodicarboxylate/triphenylphosphine (Sigma) and deprotected by hydrazine (Sigma) in dichloromethane. To substitute amine groups into thiol groups (SH), the resulting 4arm-PEG-amine was reacted with thioglycolic acid in toluene catalyzed by toluenesulfonic acid (Sigma) at 160 °C overnight. The resulting 4-arm PEG-thiol products was precipitated in cold ethyl ether. Both gelatin-VS and 4-arm PEG-thiol were dialyzed against DI water for 2 days and lyophilized before use.

5.2. Mechanical stiffness measurement of acellular gelatin hydrogels

To construct acellular gelatin hydrogels with three different mechanical stiffness and degradation rates, crosslinking density of gelatin hydrogels was tuned. Specifically, 3% (w/v) of one of gelatin-VS (low, intermediate, or high VS substituted gelatin) was cross-linked with 2% (w/v) PEG-SH. To test mechanical stiffness of the hydrogels, unconfined compression tests were conducted using an Instron 5944 materials testing system (Instron Corporation, Norwood, MA) fitted with a 10 N load cell (Interface Inc., Scottsdale, AZ). The test set-up consisted of custom- made aluminum compression platens lined with polytetrafluoroethylene to minimize friction. All tests were conducted in PBS solution at room temperature. Specimen diameter and thickness were measured using digital calipers and the material testing system's position read-out, respectively. Before each test, a preload of approximately 1 mN was applied. The upper platen was then lowered at a rate of 1% strain/sec to a maximum strain of 30%. Load and displacement data were recorded at 100 Hz. The compressive modulus was determined for strain ranges of 10–20% from linear curve fits of the stress vs. strain curve. For statistical analysis, four hydrogels per group, were prepared for the testing.

5.3. Degradation rate of acellular gelatin hydrogels *in vitro*

To examine degradation rate of three gelatin hydrogel groups, collagenase mediated degradation test was performed *in vitro*. Four hydrogels per each group were immersed in collagenase IV solution (Worthington, NJ, 2 U/mL in 3 mM $CaCl_2$ buffer solution) at room temperature on shaker. Weight of the hydrogels was measured at different time points (0, 15, 30, 45, 60, 90, 120 min, etc.) until complete degradation.

5.4. Reprogramming and maintenance of hiPSCs

Human peripheral blood mononuclear cells were reprogrammed into hiPSCs using a Sendai virus vector as previously described[54]. The obtained hiPSC clones were isolated and cultured on 6-well tissue culture plates (Greiner) coated with growth factor-reduced Matrigel (Corning). E8 pluripotent stem cell culture medium (Life Technologies) was used for hiPSC maintenance.

5.5. Differentiation of hiPSCs into hiPSC-CMs

Once a confluency of ~80–90% in the hiPSC culture was achieved, the cells were induced to differentiate into human CMs in a chemically-defined manner by using CDM3 culture media (RPMI 1640, recombinant human albumin, ascorbic acid) with a cocktail of small

molecules[12]. Briefly, differentiation was started by treating hiPSCs with a small molecule inhibitor of GSK3B signaling, CHIR99021, in CDM3 media for 2 days. The cells were subsequently treated with CDM3 media supplemented with a Wnt signaling inhibitor, Wnt-C59, for another 2 days. At days 4–8 of differentiation, CDM3 media without any factors was used and changed every other day. To improve the CM purity, cells underwent glucose starvation by culturing in CDM3 media without glucose, supplemented with 5 mM sodium DL-lactate, for 4 days[55].

5.6. Encapsulation and culture of hiPSC-CMs in gelatin hydrogels

hiPSC-CMs were dissociated into single cells using TrypLE (Life Technologies, MA) for 5–10 minutes. Then, cells were filtered using 70 μm strainer (Falcon, NY), counted, and 2.25 M cells were centrifuged at 1,300 rpm for 5 min. The cells were resuspended in 2.86% (w/v) of PEG-SH solution and kept on ice. 12.6 μL of hiPSC-CM-containing PEG solution was mixed with 5.4 μL of either low, intermediate, or high VS-functionalized gelatin solution (10% (w/v)) to achieve final concentration of 2% (w/v) PEG, 3% (w/v) gelatin, and cell (125M cells/mL). To construct microtissues, 4 μL of the mixed precursor solutions were quickly dispensed onto glass slides. The hydrogels were flattened by sandwiching Teflon plate and the glass slide with a spacer (~ 200 μm), and incubated at 37°C for 30 mins for complete gelation. After the gelation, the hydrogels were immersed in CDM3 media with FBS (10%) and rock-inhibitor, Y-27632 (Abcam, MA, ab120129, 10 μM) overnight. On the following day, the media was changed to fresh CDM3 media only with Y-27632, and replaced with it every other day.

5.7. Cell viability

To test cytotoxicity of the materials and encapsulation process, LIVE/DEAD™ Viability/ Cytotoxicity Kit (ThermoFischer Scientific, MA, L-3224) was used according to manufacturer's protocol. Briefly, calcein-AM (live dye) and ethidium homodimer-1 (dead dye) were diluted in PBS to achieve final concentration of 2 μM and 4 μM, respectively. Cell-containing hydrogels were immersed in the live/dead dye-containing PBS for 30 mins at 37°C on shaker, followed by imaging under fluorescent microscope.

5.8. Immunohistochemistry

Cells were fixed by incubating with 4% paraformaldehyde/PBS for 1 h at room temperature, washed with washing buffer (0.1% Tween–20/PBS) for 1 h once, and washed/permeabilized with 0.1% Triton X-100/PBS for 1 h at room temperature twice. Cells were blocked with a blocking buffer (3% BSA/2% goat serum/PBS) for 1 h at room temperature. Cells were incubated with primary antibodies/blocking buffer (mouse smooth muscle myosin heavy chain (SM-MHC), Abcam ab683, 1:50; rabbit collagen I, Abcam ab3,4710, 1:100; rabbit collagen IV, Abcam ab6,586, 1:100) overnight at 48C on shaker. Cells were washed with washing buffer for 1 h at room temperature three times, then incubated with secondary antibodies/Hoechst dye/blocking buffer (Alexa 488 goat-antimouse, Invitrogen A1,1001, 1:300; rhodamine goat–antirabbit, Millipore AP132, 1:300; Hoechst dye, Cell Signaling Technology 4,082S, 2 μg/mL) for 1 h at room temperature on shaker. For cytoskeletal staining, cells were incubated with Rhodamine phalloidin (Sigma P1951, 1:100 in blocking buffer) for 1 h at room temperature. Cells were again washed with washing buffer for 1 h

three times, followed by imaging using confocal microscope (oil immersion, Leica SP8 confocal system). Images were colored and overlaid using Fiji software.

5.9. Imaging-based functionality quantification

To quantify functionality of hiPSC-CMs within three hydrogel groups, video was recorded for 10 – 20s using bright field image microscope (n=3 per group). To calculate displacement field of the beating hiPSC-CMs, images were extracted at 10 fps from the video, followed by image analysis using open source Matlab PIVlab application. To validate displacement field, video and heat map graph of the displacement field were created side-by-side for comparison using Matlab. From the displacement field, the following parameters were calculated using Matlab: maximum contraction/relaxation velocity, interval between contraction-relaxation, beating per minute (BPM), and maximum contraction/relaxation stress ($\sigma = E \times \varepsilon$, E: hydrogel compressive modulus).

5.10. Statistical analysis

All samples were prepared in three or four replicates as indicated in the figure legend, and data are presented as mean ± SEM. All statistical analysis was assessed using a one-way ANOVA with Tukey's post hoc evaluation at 95% confidence interval. For all comparisons, $P < 0.05$ was considered statistically significant.

Supplementary Material

Refer to Web version on PubMed Central for supplementary material.

Acknowledgments

References

1. M. Writing Group; Mozaffarian D, Benjamin EJ, Go AS, Arnett DK, Blaha MJ, Cushman M, Das SR, de Ferranti S, Despres JP, Fullerton HJ, Howard VJ, Huffman MD, Isasi CR, Jimenez MC, Judd SE, Kissela BM, Lichtman JH, Lisabeth LD, Liu S, Mackey RH, Magid DJ, McGuire DK, Mohler ER 3rd, Moy CS, Muntner P, Mussolino ME, Nasir K, Neumar RW, Nichol G, Palaniappan L, Pandey DK, Reeves MJ, Rodriguez CJ, Rosamond W, Sorlie PD, Stein J, Towfighi A, Turan TN, Virani SS, Woo D, Yeh RW, Turner MB, C. American Heart Association Statistics, S. Stroke Statistics. Heart Disease and Stroke Statistics-2016 Update: A Report From the American Heart Association. Circulation. 2016; 133(4):e38–60. [PubMed: 26673558]

2. Langer R, Vacanti JP. Tissue engineering. Science. 1993; 260(5110):920–6. [PubMed: 8493529]

3. Nugent HM, Edelman ER. Tissue engineering therapy for cardiovascular disease. Circulation research. 2003; 92(10):1068–78. [PubMed: 12775655]

4. Li L, Chen X, Wang WE, Zeng C. How to Improve the Survival of Transplanted Mesenchymal Stem Cell in Ischemic Heart? Stem Cells Int. 2016; 2016:9682757. [PubMed: 26681958]

5. Li ZQ, Zhang M, Jing YZ, Zhang WW, Liu Y, Cui LJ, Yuan L, Liu XZ, Yu X, Hu TS. The clinical study of autologous peripheral blood stem cell transplantation by intracoronary infusion in patients with acute myocardial infarction (AMI). Int J Cardiol. 2007; 115(1):52–6. [PubMed: 16822566]

6. Schachinger V, Assmus B, Britten MB, Honold J, Lehmann R, Teupe C, Abolmaali ND, Vogl TJ, Hofmann WK, Martin H, Dimmeler S, Zeiher AM. Transplantation of progenitor cells and regeneration enhancement in acute myocardial infarction: final one-year results of the TOPCARE-AMI Trial. Journal of the American College of Cardiology. 2004; 44(8):1690–9. [PubMed: 15489105]

7. Serpooshan V, Wu SM. Patching up broken hearts: cardiac cell therapy gets a bioengineered boost. Cell stem cell. 2014; 15(6):671–3. [PubMed: 25479741]

8. Schachinger V, Erbs S, Elsasser A, Haberbosch W, Hambrecht R, Holschermann H, Yu J, Corti R, Mathey DG, Hamm CW, Suselbeck T, Werner N, Haase J, Neuzner J, Germing A, Mark B, Assmus B, Tonn T, Dimmeler S, Zeiher AM, R.-A. Investigators. Improved clinical outcome after intracoronary administration of bone-marrow-derived progenitor cells in acute myocardial infarction: final 1-year results of the REPAIR-AMI trial. Eur Heart J. 2006; 27(23):2775–83. [PubMed: 17098754]

9. Wei H, Ooi TH, Tan G, Lim SY, Qian L, Wong P, Shim W. Cell delivery and tracking in post-myocardial infarction cardiac stem cell therapy: an introduction for clinical researchers. Heart Fail Rev. 2010; 15(1):1–14. [PubMed: 19238541]

10. Zhang M, Methot D, Poppa V, Fujio Y, Walsh K, Murry CE. Cardiomyocyte grafting for cardiac repair: graft cell death and anti-death strategies. Journal of molecular and cellular cardiology. 2001; 33(5):907–21. [PubMed: 11343414]

11. Guo Y, Zhang XZ, Wei Y, Guo C, Li RX, Zeng QC, Zhang YJ. Culturing of ventricle cells at high density and construction of engineered cardiac cell sheets without scaffold. Int Heart J. 2009; 50(5):653–62. [PubMed: 19809213]

12. Burridge PW, Matsa E, Shukla P, Lin ZC, Churko JM, Ebert AD, Lan F, Diecke S, Huber B, Mordwinkin NM, Plews JR, Abilez OJ, Cui B, Gold JD, Wu JC. Chemically defined generation of human cardiomyocytes. Nature methods. 2014; 11(8):855–60. [PubMed: 24930130]

13. Nunes SS, Miklas JW, Liu J, Aschar-Sobbi R, Xiao Y, Zhang B, Jiang J, Masse S, Gagliardi M, Hsieh A, Thavandiran N, Laflamme MA, Nanthakumar K, Gross GJ, Backx PH, Keller G, Radisic M. Biowire: a platform for maturation of human pluripotent stem cell-derived cardiomyocytes. Nature methods. 2013; 10(8):781–7. [PubMed: 23793239]

14. Wendel JS, Ye L, Tao R, Zhang J, Zhang J, Kamp TJ, Tranquillo RT. Functional Effects of a Tissue-Engineered Cardiac Patch From Human Induced Pluripotent Stem Cell-Derived Cardiomyocytes in a Rat Infarct Model. Stem Cells Transl Med. 2015; 4(11):1324–32. [PubMed: 26371342]

15. Tulloch NL, Muskheli V, Razumova MV, Korte FS, Regnier M, Hauch KD, Pabon L, Reinecke H, Murry CE. Growth of engineered human myocardium with mechanical loading and vascular coculture. Circulation research. 2011; 109(1):47–59. [PubMed: 21597009]

16. Engler AJ, Griffin MA, Sen S, Bonnemann CG, Sweeney HL, Discher DE. Myotubes differentiate optimally on substrates with tissue-like stiffness: pathological implications for soft or stiff microenvironments. The Journal of cell biology. 2004; 166(6):877–87. [PubMed: 15364962]

17. Engler AJ, Carag-Krieger C, Johnson CP, Raab M, Tang HY, Speicher DW, Sanger JW, Sanger JM, Discher DE. Embryonic cardiomyocytes beat best on a matrix with heart-like elasticity: scar-like rigidity inhibits beating. J Cell Sci. 2008; 121(Pt 22):3794–802. [PubMed: 18957515]

18. Heo J, Koh RH, Shim W, Kim HD, Yim HG, Hwang NS. Riboflavin-induced photo-crosslinking of collagen hydrogel and its application in meniscus tissue engineering. Drug Deliv Transl Res. 2016; 6(2):148–58. [PubMed: 25809935]

19. Duong H, Wu B, Tawil B. Modulation of 3D fibrin matrix stiffness by intrinsic fibrinogen-thrombin compositions and by extrinsic cellular activity. Tissue Eng Part A. 2009; 15(7):1865–76. [PubMed: 19309239]

20. Liu J, Tan Y, Zhang H, Zhang Y, Xu P, Chen J, Poh YC, Tang K, Wang N, Huang B. Soft fibrin gels promote selection and growth of tumorigenic cells. Nature materials. 2012; 11(8):734–41. [PubMed: 22751180]

21. Bax NA, van Marion MH, Shah B, Goumans MJ, Bouten CV, van der Schaft DW. Matrix production and remodeling capacity of cardiomyocyte progenitor cells during in vitro differentiation. Journal of molecular and cellular cardiology. 2012; 53(4):497–508. [PubMed: 22820459]

22. Zhang B, Montgomery M, Chamberlain MD, Ogawa S, Korolj A, Pahnke A, Wells LA, Masse S, Kim J, Reis L, Momen A, Nunes SS, Wheeler AR, Nanthakumar K, Keller G, Sefton MV, Radisic M. Biodegradable scaffold with built-in vasculature for organ-on-a-chip engineering and direct surgical anastomosis. Nature materials. 2016; 15(6):669–78. [PubMed: 26950595]

23. Amano Y, Nishiguchi A, Matsusaki M, Iseoka H, Miyagawa S, Sawa Y, Seo M, Yamaguchi T, Akashi M. Development of vascularized iPSC derived 3D-cardiomyocyte tissues by filtration Layer-by-Layer technique and their application for pharmaceutical assays. Acta biomaterialia. 2016; 33:110–21. [PubMed: 26821339]

24. Reis LA, Chiu LL, Liang Y, Hyunh K, Momen A, Radisic M. A peptide-modified chitosan-collagen hydrogel for cardiac cell culture and delivery. Acta biomaterialia. 2012; 8(3):1022–36. [PubMed: 22155066]

25. Mason BN, Starchenko A, Williams RM, Bonassar LJ, Reinhart-King CA. Tuning three-dimensional collagen matrix stiffness independently of collagen concentration modulates endothelial cell behavior. Acta biomaterialia. 2013; 9(1):4635–44. [PubMed: 22902816]

26. Serpooshan V, Zhao M, Metzler SA, Wei K, Shah PB, Wang A, Mahmoudi M, Malkovskiy AV, Rajadas J, Butte MJ, Bernstein D, Ruiz-Lozano P. The effect of bioengineered acellular collagen patch on cardiac remodeling and ventricular function post myocardial infarction. Biomaterials. 2013; 34(36):9048–55. [PubMed: 23992980]

27. Hirt MN, Hansen A, Eschenhagen T. Cardiac tissue engineering: state of the art. Circulation research. 2014; 114(2):354–67. [PubMed: 24436431]

28. Don CW, Murry CE. Improving survival and efficacy of pluripotent stem cell-derived cardiac grafts. J Cell Mol Med. 2013; 17(11):1355–62. [PubMed: 24118766]

29. Mannhardt I, Breckwoldt K, Letuffe-Breniere D, Schaaf S, Schulz H, Neuber C, Benzin A, Werner T, Eder A, Schulze T, Klampe B, Christ T, Hirt MN, Huebner N, Moretti A, Eschenhagen T, Hansen A. Human Engineered Heart Tissue: Analysis of Contractile Force. Stem Cell Reports. 2016; 7(1):29–42. [PubMed: 27211213]

30. Delmar M, Makita N. Cardiac connexins, mutations and arrhythmias. Curr Opin Cardiol. 2012; 27(3):236–41. [PubMed: 22382502]

31. van der Velden J, Klein LJ, van der Bijl M, Huybregts MAJM, Stooker W, Witkop J, Eijsman L, Visser CA, Visser FC, Stienen GJM. Force production in mechanically isolated cardiac myocytes from human ventricular muscle tissue. Cardiovascular Research. 1998; 38(2):414–423. [PubMed: 9709402]

32. Schaaf S, Shibamiya A, Mewe M, Eder A, Stohr A, Hirt MN, Rau T, Zimmermann WH, Conradi L, Eschenhagen T, Hansen A. Human engineered heart tissue as a versatile tool in basic research and preclinical toxicology. PloS one. 2011; 6(10):e26397. [PubMed: 22028871]

33. Zimmermann WH, Schneiderbanger K, Schubert P, Didie M, Munzel F, Heubach JF, Kostin S, Neuhuber WL, Eschenhagen T. Tissue engineering of a differentiated cardiac muscle construct. Circulation research. 2002; 90(2):223–30. [PubMed: 11834716]

34. Ruan JL, Tulloch NL, Razumova MV, Saiget M, Muskheli V, Pabon L, Reinecke H, Regnier M, Murry CE. Mechanical Stress Conditioning and Electrical Stimulation Promote Contractility and Force Maturation of Induced Pluripotent Stem Cell-Derived Human Cardiac Tissue. Circulation. 2016

35. Young JL, Engler AJ. Hydrogels with time-dependent material properties enhance cardiomyocyte differentiation in vitro. Biomaterials. 2011; 32(4):1002–9. [PubMed: 21071078]

36. Young JL, Kretchmer K, Ondeck MG, Zambon AC, Engler AJ. Mechanosensitive kinases regulate stiffness-induced cardiomyocyte maturation. Scientific reports. 2014; 4:6425. [PubMed: 25236849]

37. Jacot JG, Martin JC, Hunt DL. Mechanobiology of cardiomyocyte development. J Biomech. 2010; 43(1):93–8. [PubMed: 19819458]

38. Ribeiro AJ, Ang YS, Fu JD, Rivas RN, Mohamed TM, Higgs GC, Srivastava D, Pruitt BL. Contractility of single cardiomyocytes differentiated from pluripotent stem cells depends on physiological shape and substrate stiffness. Proceedings of the National Academy of Sciences of the United States of America. 2015; 112(41):12705–10. [PubMed: 26417073]

39. Bedada FB, Chan SS, Metzger SK, Zhang L, Zhang J, Garry DJ, Kamp TJ, Kyba M, Metzger JM. Acquisition of a quantitative, stoichiometrically conserved ratiometric marker of maturation status in stem cell-derived cardiac myocytes. Stem Cell Reports. 2014; 3(4):594–605. [PubMed: 25358788]

40. Zustiak SP, Leach JB. Hydrolytically degradable poly(ethylene glycol) hydrogel scaffolds with tunable degradation and mechanical properties. Biomacromolecules. 2010; 11(5):1348–57. [PubMed: 20355705]

41. Park Y, Lutolf MP, Hubbell JA, Hunziker EB, Wong M. Bovine primary chondrocyte culture in synthetic matrix metalloproteinase-sensitive poly(ethylene glycol)-based hydrogels as a scaffold for cartilage repair. Tissue engineering. 2004; 10(3–4):515–22. [PubMed: 15165468]

42. Chawla K, Yu TB, Liao SW, Guan Z. Biodegradable and biocompatible synthetic saccharide-Peptide hydrogels for three-dimensional stem cell culture. Biomacromolecules. 2011; 12(3):560–7. [PubMed: 21302962]

43. Fredriksson K, Liu XD, Lundahl J, Klominek J, Rennard SI, Skold CM. Red blood cells increase secretion of matrix metalloproteinases from human lung fibroblasts in vitro. Am J Physiol Lung Cell Mol Physiol. 2006; 290(2):L326–33. [PubMed: 16403942]

44. Gao Q, Guo M, Zeng W, Wang Y, Yang L, Pang X, Li H, Suo Y, Jiang X, Yu C. Matrix metalloproteinase 9 secreted by hypoxia cardiac fibroblasts triggers cardiac stem cell migration in vitro. Stem Cells Int. 2015; 2015:836390. [PubMed: 25767513]

45. Gorgieva S, Kokol V. Preparation, characterization, and in vitro enzymatic degradation of chitosan-gelatine hydrogel scaffolds as potential biomaterials. Journal of biomedical materials research Part A. 2012; 100(7):1655–67. [PubMed: 22447615]

46. Zhuang H, Zheng JP, Gao H, De Yao K. In vitro biodegradation and biocompatibility of gelatin/montmorillonite-chitosan intercalated nanocomposite. J Mater Sci Mater Med. 2007; 18(5):951–7. [PubMed: 17221313]

47. Wu L, Ding J. Effects of porosity and pore size on in vitro degradation of three-dimensional porous poly(D,L-lactide-co-glycolide) scaffolds for tissue engineering. Journal of biomedical materials research Part A. 2005; 75(4):767–77. [PubMed: 16121386]

48. Wang HM, Chou YT, Wen ZH, Wang CZ, Chen CH, Ho ML. Novel biodegradable porous scaffold applied to skin regeneration. PloS one. 2013; 8(6):e56330. [PubMed: 23762223]

49. Lee S, Tong X, Yang F. The effects of varying poly(ethylene glycol) hydrogel crosslinking density and the crosslinking mechanism on protein accumulation in three-dimensional hydrogels. Acta biomaterialia. 2014; 10(10):4167–74. [PubMed: 24887284]

50. Jha AK, Tharp KM, Ye J, Santiago-Ortiz JL, Jackson WM, Stahl A, Schaffer DV, Yeghiazarians Y, Healy KE. Enhanced survival and engraftment of transplanted stem cells using growth factor sequestering hydrogels. Biomaterials. 2015; 47:1–12. [PubMed: 25682155]

51. Mizuno T, Yau TM, Weisel RD, Kiani CG, Li RK. Elastin stabilizes an infarct and preserves ventricular function. Circulation. 2005; 112(9 Suppl):I81–8. [PubMed: 16159870]

52. Kim DH, Lipke EA, Kim P, Cheong R, Thompson S, Delannoy M, Suh KY, Tung L, Levchenko A. Nanoscale cues regulate the structure and function of macroscopic cardiac tissue constructs. Proceedings of the National Academy of Sciences of the United States of America. 2010; 107(2):565–70. [PubMed: 20018748]

53. Stoehr A, Neuber C, Baldauf C, Vollert I, Friedrich FW, Flenner F, Carrier L, Eder A, Schaaf S, Hirt MN, Aksehirlioglu B, Tong CW, Moretti A, Eschenhagen T, Hansen A. Automated analysis of contractile force and Ca2+ transients in engineered heart tissue. Am J Physiol Heart Circ Physiol. 2014; 306(9):H1353–63. [PubMed: 24585781]

54. Churko JM, Burridge PW, Wu JC. Generation of human iPSCs from human peripheral blood mononuclear cells using non-integrative Sendai virus in chemically defined conditions. Methods Mol Biol. 2013; 1036:81–8. [PubMed: 23807788]

55. Tohyama S, Hattori F, Sano M, Hishiki T, Nagahata Y, Matsuura T, Hashimoto H, Suzuki T, Yamashita H, Satoh Y, Egashira T, Seki T, Muraoka N, Yamakawa H, Ohgino Y, Tanaka T, Yoichi M, Yuasa S, Murata M, Suematsu M, Fukuda K. Distinct metabolic flow enables large-scale purification of mouse and human pluripotent stem cell-derived cardiomyocytes. Cell stem cell. 2013; 12(1):127–37. [PubMed: 23168164]
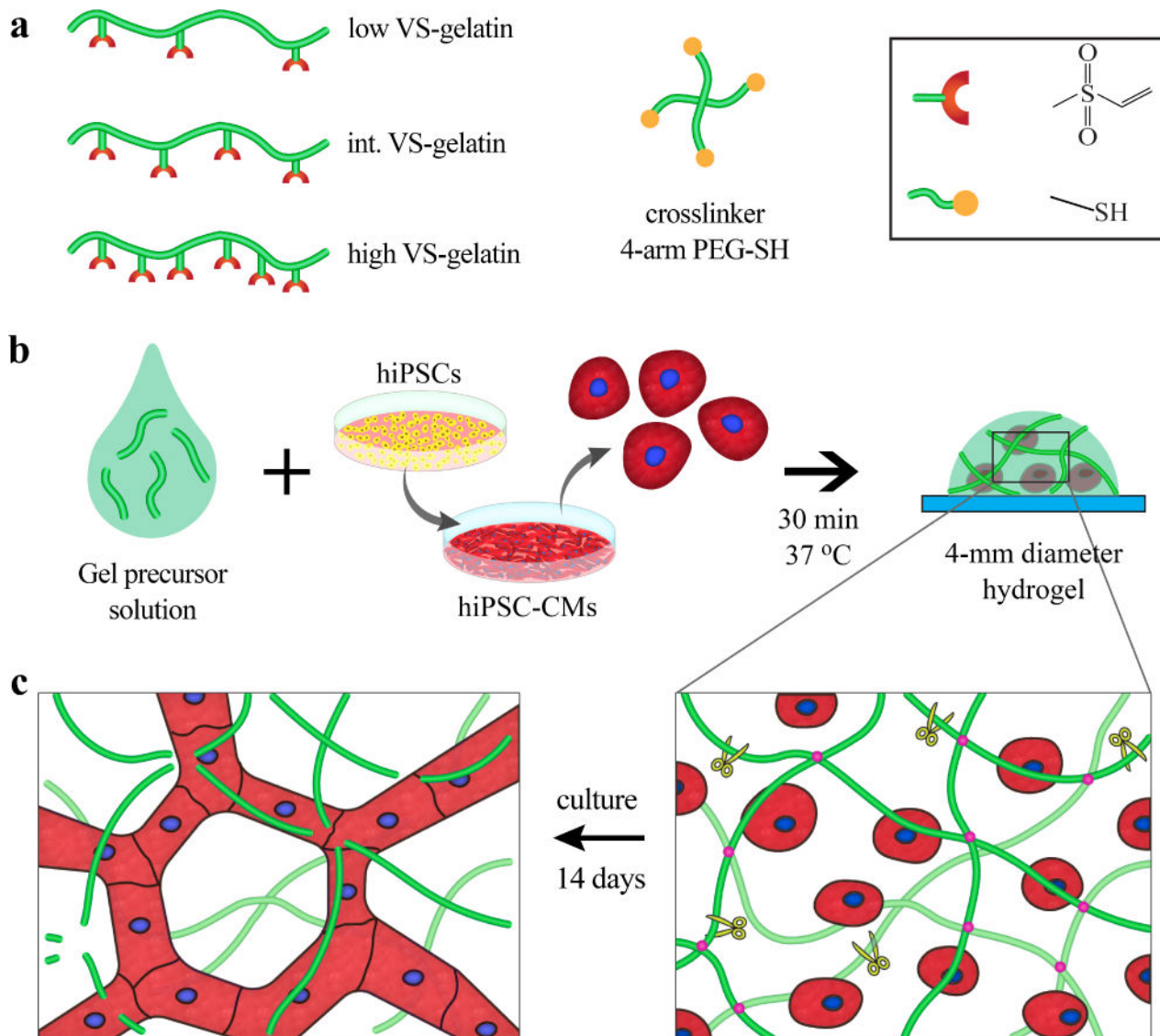
Figure 1. Schematic of experimental design
a To vary stiffness and degradation rate of gelatin hydrogels, gelatin chains were functionalized with vinyl sulfone (VS) to different degrees (low, intermediate, and high). 4-arm thiolated poly(ethylene glycol) (PEG-SH) was used as a crosslinker. **b** Human induced pluripotent stem cell-derived cardiomyocytes (hiPSC-CMs) were encapsulated at high density (125M cells/mL) to mimic the native myocardium. **c** During 14 days of culture, hiPSC-CMs degraded the gelatin matrix and formed intercellular network.
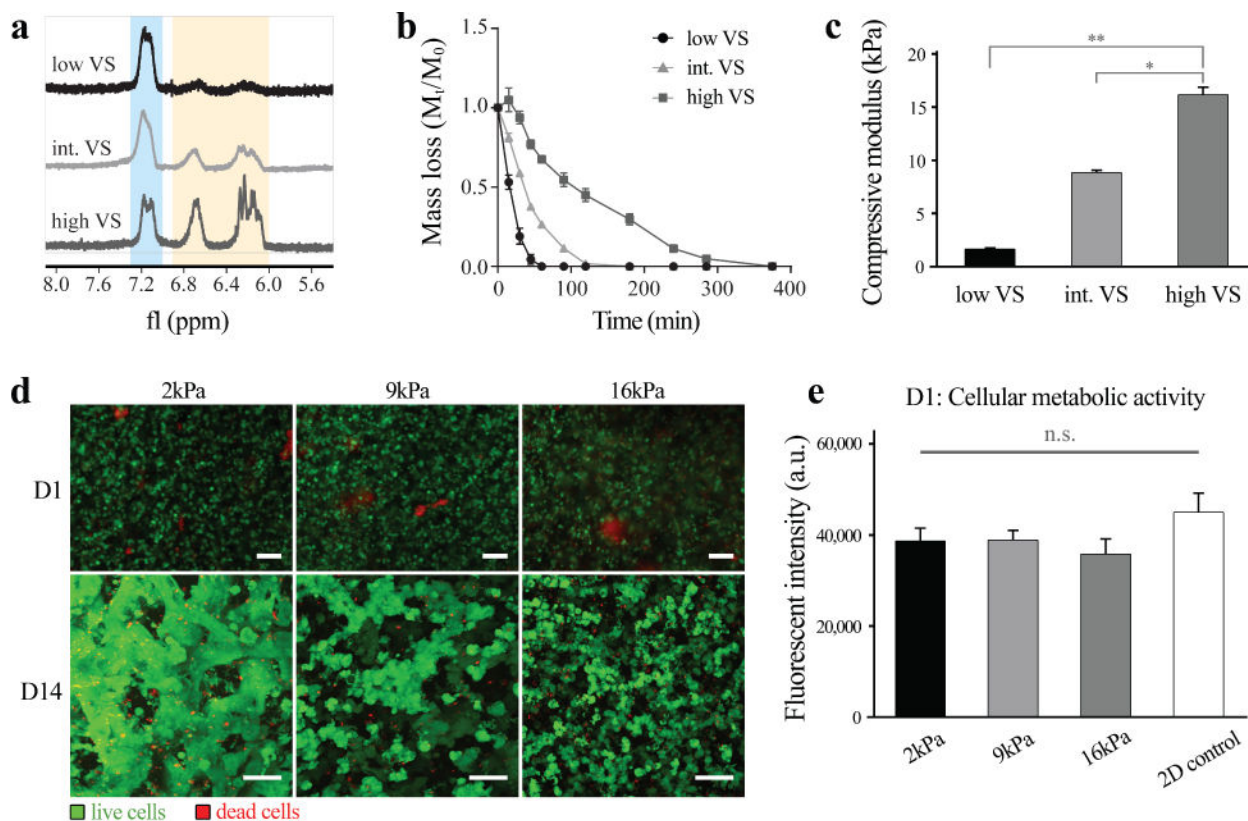
**Figure 2. Materials characterization and hiPSC-CM viability**

a ^{1}H-NMR data confirms that gelatin chains were functionalized with VS at three different degrees (low, intermediate, and high) as indicated by integral area under the peak between 6.0–6.9 ppm (orange box). The peak between 7.0–7.3 ppm was used as gelatin loading control (blue box). **b** *in vitro* degradation assay revealed that low VS-functionalized gelatin hydrogels led to the fastest hydrogel degradation (•), while high VS-functionalized gels led to the slowest degradation (■). **c** Unconfined compression test showed that increasing degree of VS functionalization led to increasing compressive modulus of gelatin hydrogels. **d** Live-Dead assay demonstrated relatively high cell viability in all three study groups over the 14-day 3D culture period. (scale bar: 100 μm) **e** AlamarBlue assay confirmed that hiPSC-CM metabolic activity in 3D hydrogels were not significantly different from that of the 2D control group at day 1 (one-way ANOVA, n.s. $p > 0.05$).
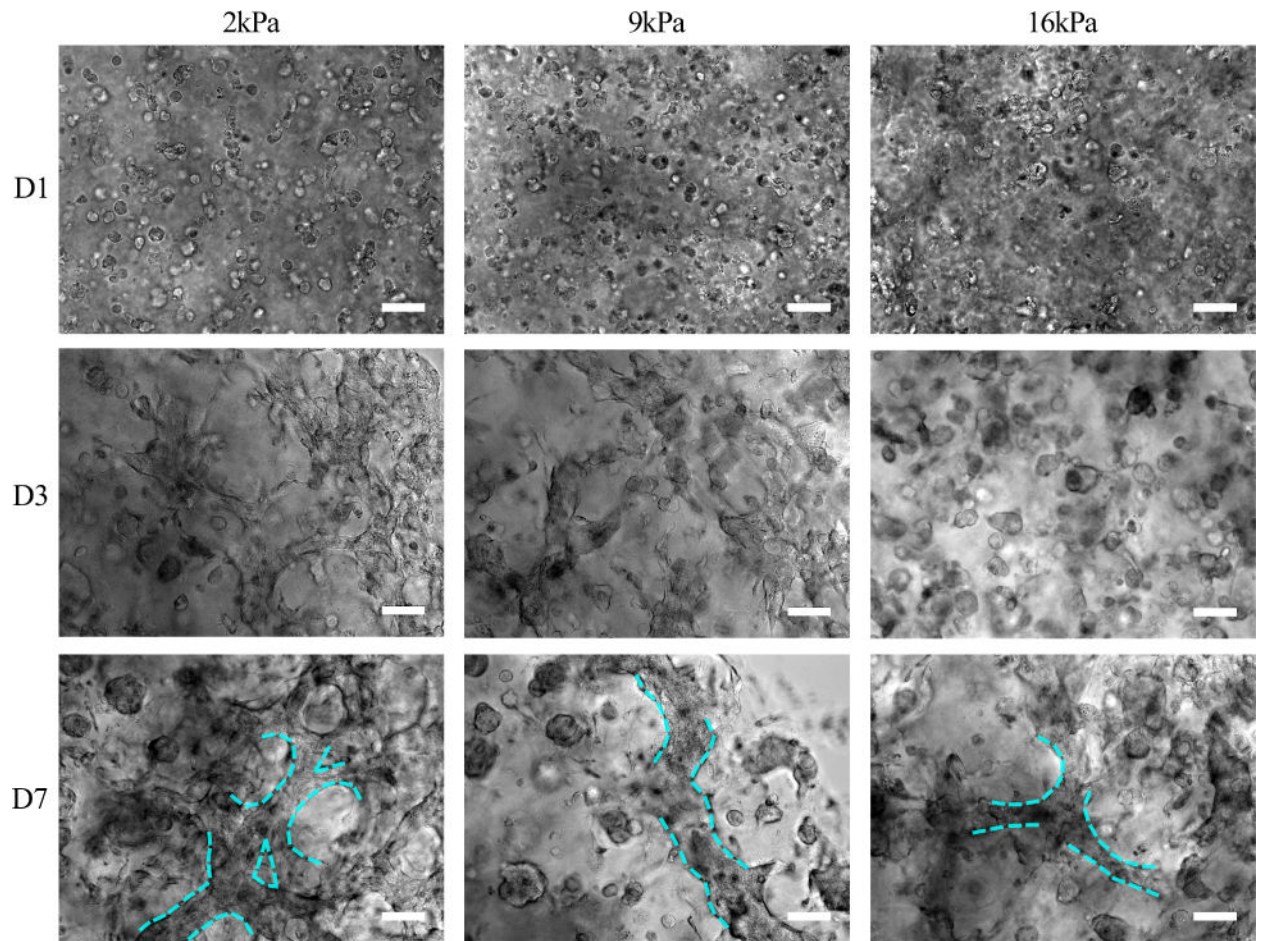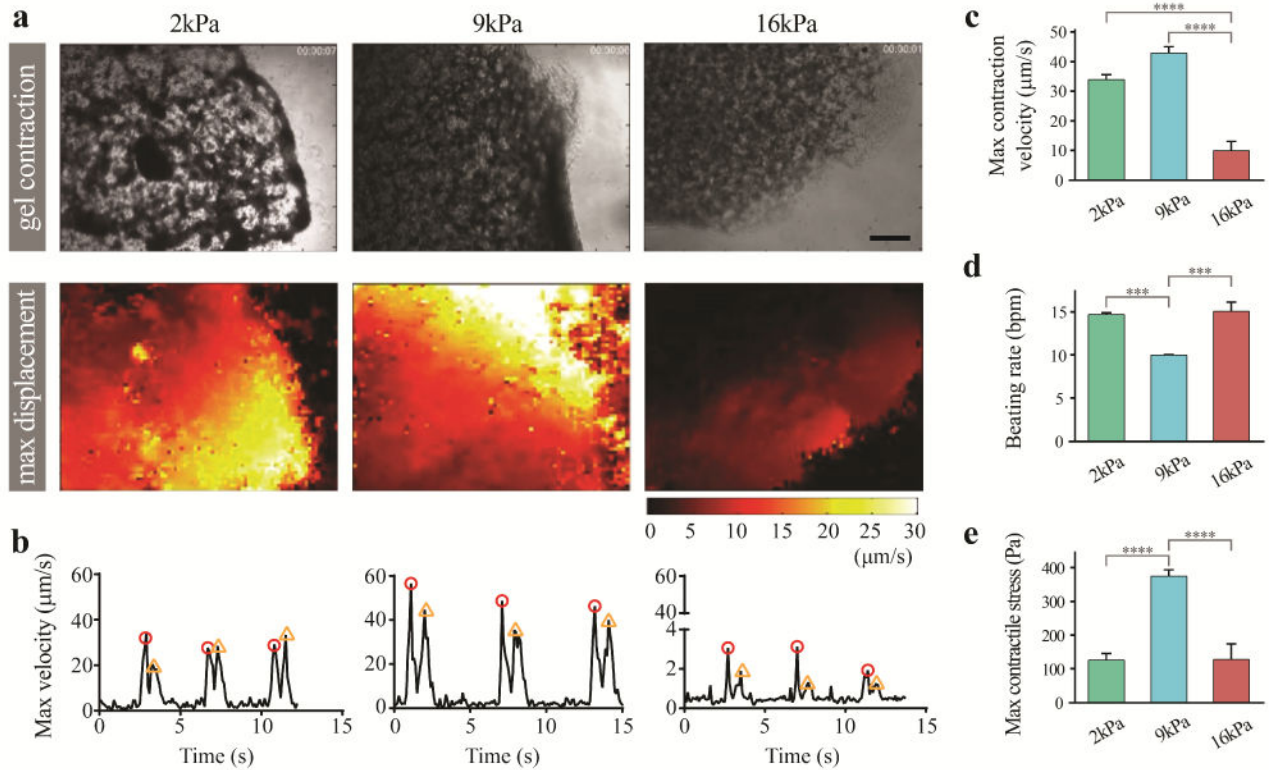
Figure 3. Effects of hydrogel degradation and stiffness on hiPSC-CM intercellular connection and network formation
Increasing degradation rate facilitated intercellular network formation. The dashed lines highlight the shape of the cellular networks. Scale bar: 50 μm.
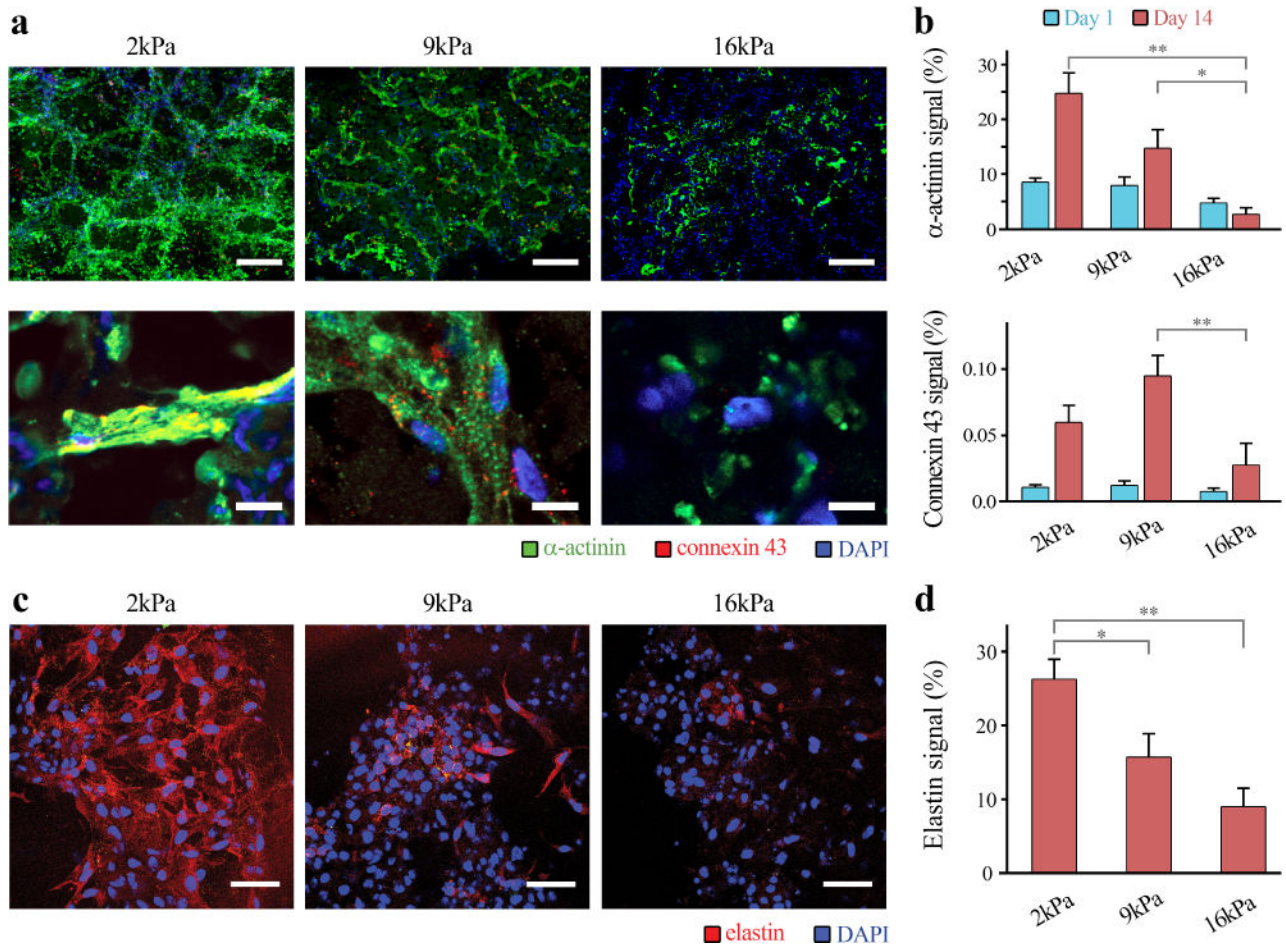
Figure 4. Effects of hydrogel degradation and stiffness on hiPSC-CM phenotype retention and *de novo* extracellular matrix production

a hiPSC-CMs cultured in 2kPa and 9kPa hydrogel groups exhibited higher expression levels of α-actinin and connexin 43, in comparison to those in 16kPa group. It is notable that only CMs in 9kPa showed evidences of organized sarcomeric α-actinin structure (Day 14, scale bar: 200 μm – top and 50 μm – bottom). **b** Quantification of α-actinin (top) and connexin 43 (bottom) levels among the 3 hydrogel groups. 2kPa and 9kPa groups demonstrated significantly greater levels of α-actinin and connexin 43 expression than the 16kPa group (two-way ANOVA, **p<0.01). **c,d** Elastin production of hiPSC-CMs was significantly facilitated with increasing degradation (decreasing stiffness) (scale bar: 50 μm, one-way ANOVA, *p<0.05, **p<0.01).

Figure 5. Effects of hydrogel degradation and stiffness on hiPSC-CM contractile function
a CM function was examined by global gel contraction behavior (top), which was recorded and converted into displacement vector field (heat maps, bottom) using computational analysis. (scale bar: 200 μm) **b** Max displacement was then plotted as a function of time (contraction peak: red circle, relaxation peak: orange triangle). **c** hiPSC-CMs in gelatin hydrogels with greater degradation rate (lower stiffness) showed significantly higher max contraction velocity in comparison to 16kPa group. **d** CMs in 2 and 16 kPa groups demonstrated significantly greater beating rates than those cultured in 9kPa groups. **e** Measurement of max contractile stress. Note that the 9 kPa group showed the greatest level of contractile stress among the 3 hydrogel groups. One-way ANOVA test was used; ***p<0.001 and ****p<0.0001.